Induced spin-triplet pairing in the coexistence state of antiferromagnetism and singlet superconductivity: Collective modes and microscopic properties

D. E. Almeida,[1,2] R. M. Fernandes,[2] and E. Miranda[1]

[1]*Instituto de Física Gleb Wataghin, Unicamp, Rua Sérgio Buarque de Holanda, 777, CEP 13083-859 Campinas, SP, Brazil*

[2]*School of Physics and Astronomy, University of Minnesota, Minnesota, Minneapolis 55455, USA*

(Received 4 May 2017; published 24 July 2017)

The close interplay between superconductivity and antiferromagnetism in several quantum materials can lead to the appearance of an unusual thermodynamic state in which both orders coexist microscopically, despite their competing nature. A hallmark of this coexistence state is the emergence of a spin-triplet superconducting gap component, called a π triplet, which is spatially modulated by the antiferromagnetic wave vector, reminiscent of a pair density wave. In this paper, we investigate the impact of these π-triplet degrees of freedom on the phase diagram of a system with competing antiferromagnetic and superconducting orders. Although we focus on a microscopic two-band model that has been widely employed in studies of iron pnictides, most of our results follow from a Ginzburg-Landau analysis, and as such should be applicable to other systems of interest, such as cuprates and heavy fermion materials. The Ginzburg-Landau functional reveals not only that the π-triplet gap amplitude couples trilinearly with the singlet gap amplitude and the staggered magnetization magnitude but also that the π-triplet d-vector couples linearly with the magnetization direction. While in the mean-field level this coupling forces the d-vector to align parallel or antiparallel to the magnetization, in the fluctuation regime it promotes two additional collective modes—a Goldstone mode related to the precession of the d-vector around the magnetization and a massive mode, related to the relative angle between the two vectors, which is nearly degenerate with a Leggett-like mode associated with the phase difference between the singlet and triplet gaps. We also investigate the impact of magnetic fluctuations on the superconducting-antiferromagnetic phase diagram, showing that due to their coupling with the π-triplet order parameter the coexistence region is enhanced. This effect stems from the fact that the π-triplet degrees of freedom promote an effective attraction between the antiferromagnetic and singlet superconducting degrees of freedom, highlighting the complex interplay between these two orders, which goes beyond mere competition for the same electronic states.

DOI: 10.1103/PhysRevB.96.014514

I. INTRODUCTION

The close proximity between the superconducting (SC) and antiferromagnetic (AFM) transitions in unconventional superconductors such as cuprates, iron pnictides, and heavy fermion compounds has motivated a profound investigation of the interplay between these two phases [1–4]. In general, these two ordered states compete for the same electronic states, as manifested for instance by the suppression of the AFM order parameter (OP) below the SC transition temperature T_c observed in neutron-diffraction experiments [5,6]. Despite this competition, these two antagonistic phases can coexist microscopically, giving rise to a new thermodynamic state in which both the U(1) gauge symmetry and the SO(3) spin-rotational symmetry are simultaneously broken. Experimentally, identifying such a microscopic coexistence phase is challenging: because bulk probes are generally sensitive not only to the order parameter but also to its volume fraction [5], it is difficult to distinguish the situation in which the two orders coexist locally from the case in which the system phase-separates into nonoverlapping domains of AFM and SC orders. As a result, local probes are generally needed to unambiguously identify the AFM-SC microscopic coexistence phase.

Recently, nuclear magnetic resonance, muon spin rotation, scanning tunneling microscopy, and Mössbauer experiments have revealed that several iron-based superconductors display this unique AFM-SC coexistence state in their phase diagrams [7–15]. Data supporting the existence of this state in certain cuprates [16] and heavy fermion systems [6,17–19] have also been reported. Thus, it is of general interest to elucidate the microscopic and macroscopic properties of the AFM-SC coexistence state, not only to provide useful benchmarks to probe it but also to search for possible novel phenomena in this unusual phase of matter.

Indeed, many theoretical works have tackled this issue and provided invaluable information about the interplay between AFM and unconventional SC in the coexistence state [20–36]. Interestingly, as shown in Ref. [37], the fact that the AFM order parameter $\boldsymbol{M}$ and the singlet SC order parameter Δ_s are simultaneously nonzero implies that a triplet component of the superconducting order parameter is generated, $\Delta_t \propto \Delta_s \boldsymbol{M}$. It is clear that this triplet component only exists in the case of microscopic AFM-SC phase coexistence, since in the case of phase separation either Δ_s or $\boldsymbol{M}$ vanishes at an arbitrary point. Consequently, detecting this triplet component, often called a π triplet (and hereafter denoted t-SC), would provide unambiguous evidence in favor of a coexistence AFM-SC state. On the microscopic level, this triplet component pairs electrons with momenta $-\boldsymbol{k}$ and $\boldsymbol{k}+\boldsymbol{Q}$, i.e.,

$$\Delta_t \propto \sum_{\boldsymbol{k}} (\hat{\boldsymbol{d}} \cdot \boldsymbol{\sigma} i\sigma^y)^{\dagger}_{ss'} \langle c_{\boldsymbol{k}+\boldsymbol{Q},s} c_{-\boldsymbol{k},s'} \rangle. \quad (1)$$

Here, $c_{\boldsymbol{k},s}$ is the standard fermionic operator associated with an electron with momentum $\boldsymbol{k}$ and spin s, σ^j are the Pauli matrices, and $\hat{\boldsymbol{d}}$ is the triplet d-vector. Since the center of mass of the Cooper pair has momentum $\boldsymbol{Q}$ equal to the AFM wave

vector, this order parameter behaves similarly to a pair density wave [38–40]. Note, however, that the term *pair density wave* has been primarily employed to describe a SC state without a homogeneous gap component, which is not possible in our case, since Δ_t only appears in the presence of a homogeneous singlet component Δ_s. Despite the fact that the system still has inversion symmetry and Δ_t has even parity, we identify Δ_t as a triplet because of its spin structure. The reason why the triplet spin structure is allowed in the AFM phase, even though Δ_t has even parity, is because inside the AFM phase $c_{\boldsymbol{k}+\boldsymbol{Q},s}$ and $c_{\boldsymbol{k},s}$ become different "electronic flavors" due to the band folding. This can be more easily visualized by rewriting the expression for the triplet gap as

$$\Delta_t \propto \frac{1}{2}\sum_{\boldsymbol{k}}(\hat{\boldsymbol{d}}\cdot\boldsymbol{\sigma}\mathrm{i}\sigma^y)^{\dagger}_{ss'}(i\tau^y)^{\mu\nu}\left\langle\Phi^{\mu}_{\mathbf{k},s}\Phi^{\mu}_{-\mathbf{k},s}\right\rangle \tag{2}$$

where $\Phi^{\mu}_{\mathbf{k},s} = (c_{\boldsymbol{k}+\boldsymbol{Q},s} \quad c_{-\boldsymbol{k},s})^T$ is a spinor in both spin space and AFM band-folded space. The situation resembles the case of multiorbital systems with atomic spin-orbit coupling $\boldsymbol{S}\cdot\boldsymbol{L}$, in which case the superconducting order parameter generally has both singlet and triplet components (although inversion symmetry is preserved) [41].

Different aspects of the impact of this π-triplet component on the AFM-SC coexistence phase have been previously discussed [37,42–48]. In most cases, the analyses focused on the ordered state, where the d-vector is fixed parallel to the magnetization direction $\hat{\boldsymbol{M}}$. In this paper, we focus instead on the disordered state, and investigate the coupling between the d-vector and the magnetization $\boldsymbol{M}$. For concreteness, we consider a microscopic two-band model widely employed to study the interplay between AFM and SC in the iron pnictide superconductors, but most of our results should hold in other systems as well. As it was previously shown in Refs. [20,21], the phase diagram of this model displays a tetracritical point and, consequently, an AFM-SC coexistence phase. Near the tetracritical point, we then use the microscopic model to derive the Ginzburg-Landau (GL) free energy in the disordered state and show that the d-vector couples linearly with $\boldsymbol{M}$. While in the ordered state this implies that the two vectors are parallel, as assumed in previous works, in the disordered state it gives rise to a collective mode corresponding to oscillations of the angle between the AFM order parameter and the d-vector of the t-SC order parameter. We find that in general this collective mode has a finite energy, which is comparable to, but larger than, the Leggett-like mode associated with oscillations of the relative phase between the singlet and triplet SC order parameters.

We then go beyond the mean-field approach and study how magnetic fluctuations modify the phase diagram. In general, we find that AFM fluctuations shrink the magnetically ordered region, as expected, while keeping the second-order character of the phase transition lines. More importantly, the t-SC order acts to expand the AFM-SC phase coexistence, by promoting an effective attraction between these two otherwise competing orders. Finally, we discuss the implications of our results to the understanding of the phase diagrams of unconventional superconductors.

The paper is organized as follows. In Sec. II we present our microscopic model and derive the Ginzburg-Landau functional. The mean-field phase diagram and the analysis of the corresponding collective modes are shown in Sec. III. Section IV is devoted to the investigation of the effects of magnetic fluctuations. Concluding remarks are presented in Sec. V. Two appendices contain additional technical details of the derivations discussed in the main text.

II. MICROSCOPIC MODEL AND THE GINZBURG-LANDAU FUNCTIONAL

A. The model

We consider a two-dimensional two-band model containing one hole band and one electron band. Such a model has been widely employed in studies of the interplay between SC and AFM in iron pnictides; see for instance Refs. [20,21]. While this model is useful to obtain microscopic values for the Ginzburg-Landau parameters, we emphasize that most of our results are quite general and apply to any other system where the AFM and SC transition lines meet at a tetracritical point. The Hamiltonian contains four terms:

$$\mathcal{H} = \mathcal{H}_0 + \mathcal{H}_{\mathrm{AFM}} + \mathcal{H}^{\mathrm{s}}_{\mathrm{SC}} + \mathcal{H}^{\mathrm{t}}_{\mathrm{SC}}. \tag{3}$$

The noninteracting part $\mathcal{H}_0$ describes the two bands, the centers of which are displaced by $\boldsymbol{Q} = (\pi,\pi)$:

$$\mathcal{H}_0 = \sum_{\boldsymbol{k},s}(\xi_{1,\boldsymbol{k}}c^{\dagger}_{\boldsymbol{k},s}c_{\boldsymbol{k},s} + \xi_{2,\boldsymbol{k}+\boldsymbol{Q}}f^{\dagger}_{\boldsymbol{k}+\boldsymbol{Q},s}f_{\boldsymbol{k}+\boldsymbol{Q},s}), \tag{4}$$

where $c^{\dagger}_{\boldsymbol{k},s}$ ($f^{\dagger}_{\boldsymbol{k}+\boldsymbol{Q},s}$) is an operator that creates a fermion with momentum $\boldsymbol{k}$ ($\boldsymbol{k}+\boldsymbol{Q}$) and spin projection $s=\pm1$. The isotropic hole-band dispersion is given by $\xi_{1,\boldsymbol{k}} = \varepsilon_{1,0} - k^2/2m - \mu$, whereas the anisotropic electron-band dispersion is $\xi_{2,\boldsymbol{k}+\boldsymbol{Q}} = -\varepsilon_{2,0} + k_x^2/2m_x + k_y^2/2m_y - \mu$. Note that the chemical potential μ has been included in the dispersions and $\varepsilon_{1,0} > 0$ and $\varepsilon_{2,0} > 0$ are offset energies. To proceed, we introduce the notation $\tan\theta = k_y/k_x$ and rewrite the band dispersions according to $\xi_{2,\boldsymbol{k}+\boldsymbol{Q}} = -\xi_{1,\boldsymbol{k}} + 2\delta_{\boldsymbol{k}}$, where $\delta_{\boldsymbol{k}} = \delta_0(k) + \delta_2(k)\cos 2\theta$ measures the deviation from the perfect nesting condition ($\xi_{1,\boldsymbol{k}} = -\xi_{2,\boldsymbol{k}+\boldsymbol{Q}}$) with $\delta_0(k) = (\varepsilon_{1,0} - \varepsilon_{2,0})/2 - \mu + k^2(m_x^{-1} + m_y^{-1} - 2m^{-1})/8$ and $\delta_2(k) = k^2(m_x^{-1} - m_y^{-1})/8$ [20].

The second term of the Hamiltonian describes the repulsive interactions that drive AFM in the presence of (im)perfect nesting with vector $\boldsymbol{Q}$:

$$\mathcal{H}_{\mathrm{AFM}} = -\frac{V_{\mathrm{m}}}{2\upsilon}\sum_{\boldsymbol{k},\boldsymbol{k}'}(c^{\dagger}_{\boldsymbol{k},s}\boldsymbol{\sigma}_{ss'}f_{\boldsymbol{k}+\boldsymbol{Q},s'})\cdot(f^{\dagger}_{\boldsymbol{k}'+\boldsymbol{Q},\sigma}\boldsymbol{\sigma}_{\sigma\sigma'}c_{\boldsymbol{k}',\sigma'}), \tag{5}$$

where υ is the volume of the system, V_{m} is the coupling constant (the momentum dependence of which we dropped, for simplicity), and $\boldsymbol{\sigma}_{ss'}$ is the (ss') element of the Pauli matrix vector. Hereafter, repeated spin indices are implicitly summed over.

The fermions are also subject to interband pairing interactions, both in the singlet and in the triplet channels, which are described, respectively, by the two last terms in $\mathcal{H}$:

$$\mathcal{H}^{\mathrm{s}}_{\mathrm{SC}} = -\frac{V_{\mathrm{s}}}{2\upsilon}\sum_{\boldsymbol{k},\boldsymbol{k}'}[(\mathrm{i}\sigma^y)_{ss'}(\mathrm{i}\sigma^y)^{\dagger}_{\sigma\sigma'} \times (c^{\dagger}_{\boldsymbol{k},s}c^{\dagger}_{-\boldsymbol{k},s'}f_{-\boldsymbol{k}'-\boldsymbol{Q},\sigma}f_{\boldsymbol{k}'+\boldsymbol{Q},\sigma'}) + \mathrm{H.c.}] \tag{6}$$

and

$$\mathcal{H}^{\rm t}_{\rm SC} = -\frac{V_{\rm t}}{2\upsilon}\sum_{\boldsymbol{k},\boldsymbol{k}'}[(\hat{\boldsymbol{d}}\cdot\boldsymbol{\sigma}\mathrm{i}\sigma^y)_{ss'}(\hat{\boldsymbol{d}}\cdot\boldsymbol{\sigma}\mathrm{i}\sigma^y)^\dagger_{\sigma\sigma'} \times (f^\dagger_{\boldsymbol{k}+\boldsymbol{Q},s}c^\dagger_{-\boldsymbol{k},s'}c_{-\boldsymbol{k}',\sigma}f_{\boldsymbol{k}'+\boldsymbol{Q},\sigma'}) + \text{H.c.}], \quad (7)$$

where $V_{\rm s}$ and $V_{\rm t}$ are the singlet and triplet SC couplings, respectively. The triplet SC pairs have a finite momentum $\boldsymbol{Q}$, and are characterized by the unitary d-vector $\hat{\boldsymbol{d}} = (\hat{d}_x,\hat{d}_y,\hat{d}_z)^T$. The spinor $\hat{\boldsymbol{d}}\cdot\boldsymbol{\sigma}\mathrm{i}\sigma^y$ for triplet Cooper pairs is discussed in Refs. [49–51] (see also Refs. [37,44]). We follow Ref. [43] and include from the beginning the triplet component because, when the rotational symmetry in spin space is broken and the system undergoes a singlet SC phase transition, triplet components $\langle c_{-\boldsymbol{k},s}f_{\boldsymbol{k}+\boldsymbol{Q},s'}\rangle$ are necessarily generated.

We now define the various OPs. The staggered magnetization is

$$\boldsymbol{M} = -\frac{V_{\rm m}}{2\upsilon}\sum_{\boldsymbol{k}}\boldsymbol{\sigma}_{ss'}\langle f^\dagger_{\boldsymbol{k}+\boldsymbol{Q},s}c_{\boldsymbol{k},s'}\rangle, \quad (8)$$

the singlet SC OPs for each band are

$$\Delta_{\rm s,1} = -\frac{V_{\rm s}}{\upsilon}\sum_{\boldsymbol{k}}\langle f_{\boldsymbol{k}+\boldsymbol{Q},\uparrow}f_{-\boldsymbol{k}-\boldsymbol{Q},\downarrow}\rangle, \quad (9)$$

$$\Delta_{\rm s,2} = -\frac{V_{\rm s}}{\upsilon}\sum_{\boldsymbol{k}}\langle c_{\boldsymbol{k},\uparrow}c_{-\boldsymbol{k},\downarrow}\rangle, \quad (10)$$

and the triplet SC OP is [37,44,49,50]

$$\Delta_{\rm t} = -\frac{V_{\rm t}}{2\upsilon}\sum_{\boldsymbol{k}}\langle f_{\boldsymbol{k}+\boldsymbol{Q},s}(\hat{\boldsymbol{d}}\cdot\boldsymbol{\sigma}\mathrm{i}\sigma^y)^\dagger_{ss'}c_{-\boldsymbol{k},s'}\rangle. \quad (11)$$

We use the usual mean-field decoupling to rewrite the quartic terms of $\mathcal{H}$ as

$$\mathcal{H}_{\rm AFM} \approx \sum_{\boldsymbol{k}}[c^\dagger_{\boldsymbol{k},s}(\boldsymbol{M}\cdot\boldsymbol{\sigma})_{ss'}f_{\boldsymbol{k}+\boldsymbol{Q},s'} + \text{H.c.}], \quad (12)$$

$$\mathcal{H}^{\rm s}_{\rm SC} \approx \sum_{\boldsymbol{k}}(\Delta_{\rm s,1}c^\dagger_{\boldsymbol{k},\uparrow}c^\dagger_{-\boldsymbol{k},\downarrow} + \Delta_{\rm s,2}f^\dagger_{\boldsymbol{k}+\boldsymbol{Q},\uparrow}f^\dagger_{-\boldsymbol{k}-\boldsymbol{Q},\downarrow} + \text{H.c.}) \quad (13)$$

and

$$\mathcal{H}^{\rm t}_{\rm SC} \approx -\frac{1}{2}\sum_{\boldsymbol{k}}[(\hat{\Delta}_{\rm t})_{ss'}(f^\dagger_{\boldsymbol{k}+\boldsymbol{Q},s}c^\dagger_{-\boldsymbol{k},s'} - c^\dagger_{\boldsymbol{k},s}f^\dagger_{-\boldsymbol{k}-\boldsymbol{Q},s'}) + \text{H.c.}], \quad (14)$$

where we introduced the notation $(\hat{\Delta}_{\rm t})_{ss'} = (\hat{\boldsymbol{d}}\cdot\boldsymbol{\sigma}\mathrm{i}\sigma^y)_{ss'}\Delta_{\rm t}$ and we also omitted the constant terms for simplicity. Note that the singlet SC gap of one band is due to the action of the electrons in the other band and that the triplet SC OP has a finite momentum $\boldsymbol{Q}$. To proceed, we introduce the eight-component Balian-Werthamer spinor $\psi^\dagger_{\boldsymbol{k}} = (c^\dagger_{\boldsymbol{k},\uparrow},c^\dagger_{\boldsymbol{k},\downarrow},c_{-\boldsymbol{k},\uparrow},c_{-\boldsymbol{k},\downarrow},f^\dagger_{\boldsymbol{k}+\boldsymbol{Q},\uparrow},f^\dagger_{\boldsymbol{k}+\boldsymbol{Q},\downarrow},f_{-\boldsymbol{k}-\boldsymbol{Q},\uparrow},f_{-\boldsymbol{k}-\boldsymbol{Q},\downarrow})$ to write the total Hamiltonian in compact form as

$$\mathcal{H}_{\rm MF} = \frac{1}{2}\sum_{\boldsymbol{k}}\psi^\dagger_{\boldsymbol{k}}\hat{H}_{\boldsymbol{k}}\psi_{\boldsymbol{k}} + E_{\rm cond}, \quad (15)$$

where $E_{\rm cond} = 2\upsilon[\frac{\boldsymbol{M}^2}{V_{\rm m}} - \frac{\mathrm{Re}(\Delta_{\rm s,1}\Delta^*_{\rm s,2})}{V_{\rm s}} + \frac{|\Delta_{\rm t}|^2}{V_{\rm t}}]$ contains the constant terms omitted above and

$$\hat{H}_{\boldsymbol{k}} = \begin{bmatrix} \xi_{1,\boldsymbol{k}}\mathbb{1}_2 & \Delta_{\rm s,1}(i\sigma^y) & \boldsymbol{M}\cdot\boldsymbol{\sigma} & \hat{\Delta}_{\rm t} \\ -\Delta^*_{\rm s,1}(i\sigma^y) & -\xi_{1,\boldsymbol{k}}\mathbb{1}_2 & -\hat{\Delta}^\dagger_{\rm t} & -(\boldsymbol{M}\cdot\boldsymbol{\sigma}) \\ (\boldsymbol{M}\cdot\boldsymbol{\sigma})^T & -\hat{\Delta}_{\rm t} & \xi_{2,\boldsymbol{k}+\boldsymbol{Q}}\mathbb{1}_2 & \Delta_{\rm s,2}(i\sigma^y) \\ \hat{\Delta}^\dagger_{\rm t} & -(\boldsymbol{M}\cdot\boldsymbol{\sigma})^T & -\Delta^*_{\rm s,2}(i\sigma^y) & -\xi_{2,\boldsymbol{k}+\boldsymbol{Q}}\mathbb{1}_2 \end{bmatrix}. \quad (16)$$

Note that we have omitted the constant term $\frac{1}{2}\sum_{\boldsymbol{k}}(\xi_{1,\boldsymbol{k}} + \xi_{2,\boldsymbol{k}+\boldsymbol{Q}})$ in Eq. (15).

Because $\boldsymbol{Q}$ is commensurate and $2\boldsymbol{Q}$ is a reciprocal-lattice vector, the magnetic OP $\boldsymbol{M}$ is real. Furthermore, we assume that $V_s > 0$, implying that the SC gaps are of equal magnitude but different signs in the two bands, $\Delta_{\rm s,2} = -\Delta_{\rm s,1} = \Delta_{\rm s}$, as discussed in Ref. [21]. This is the so-called s^{+-} superconducting state. As usual, the gaps are parametrized by their magnitude and phases, $\Delta_{\rm s} = |\Delta_{\rm s}|e^{\mathrm{i}\alpha_{\rm s}}$ and $\Delta_{\rm t} = |\Delta_{\rm t}|e^{\mathrm{i}(\alpha_{\rm s}-\alpha_{\rm st})}$. Note that, in the present analysis, we will ignore modes associated with the relative phase between the two gaps of the two bands—such modes usually have high energies when the pairing interaction is dominated by interband processes, as in our case [52]. Furthermore, they are absent in single band systems with a d-wave gap, for which the present analysis can be extended in a straightforward way.

B. Derivation of the free energy

The model discussed above was previously shown to display an AFM-SC tetracritical point, for a wide range of band dispersion parameters [20,21] (note that in the case of conventional s^{++} SC the phase diagram has only a bicritical point and no AFM-SC coexistence). The Ginzburg-Landau free energy can be obtained in a straightforward way by integrating out the fermionic fields of the quadratic mean-field Hamiltonian [Eq. (15)], yielding (for an alternative approach to obtain a similar GL functional, see Ref. [47])

$$F = E_{\rm cond} - \frac{\upsilon}{2}\int_k \ln\left[\det\left(-\hat{\mathcal{G}}^{-1}_k\right)\right], \quad (17)$$

where the Green's function is given by $\hat{\mathcal{G}}^{-1}_k = \mathrm{i}\omega_n - \hat{H}_{\boldsymbol{k}}$, $\omega_n = (2n+1)\pi T$ is a fermionic Matsubara frequency ($n = 0, \pm 1, \pm 2, \ldots$), the determinant is over the Balian-Werthamer indices, and $\int_k = T\sum_{\omega_n}\frac{1}{\upsilon}\sum_{\boldsymbol{k}}$. For simplicity, we introduced the short notation $k = (\boldsymbol{k},\omega_n)$. Performing the matrix operations, we find

$$f(\boldsymbol{M},\Delta_{\rm s},\Delta_{\rm t}) = -\int_k \ln\left[\left(\omega_n^2 + E^2_{+,\boldsymbol{k}}\right)\left(\omega_n^2 + E^2_{-,\boldsymbol{k}}\right)\right] + \frac{2\boldsymbol{M}^2}{V_{\rm m}} + \frac{2|\Delta_{\rm s}|^2}{V_{\rm s}} + \frac{2|\Delta_{\rm t}|^2}{V_{\rm t}}, \quad (18)$$

where $f = F/\upsilon$ is the free-energy density and $E^2_{\pm,\boldsymbol{k}} = \Gamma_{\boldsymbol{k}} \pm \Omega_{\boldsymbol{k}}$ are the squares of the eigenenergies of the reduced Hamiltonian [Eq. (16)], with

$$\Gamma_{\boldsymbol{k}} = |\Delta_{\rm s}|^2 + |\Delta_{\rm t}|^2 + \boldsymbol{M}^2 + \left(\xi^2_{2,\boldsymbol{k}+\boldsymbol{Q}} + \xi^2_{1,\boldsymbol{k}}\right)/2, \quad (19)$$

and

$$\Omega_{\boldsymbol{k}}^2 = [2|\Delta_s||\Delta_t|\hat{\boldsymbol{d}}\cos\alpha_{st} + \boldsymbol{M}(\xi_{2,\boldsymbol{k}+\boldsymbol{Q}} + \xi_{1,\boldsymbol{k}})]^2 + |\Delta_t|^2(\xi_{1,\boldsymbol{k}} - \xi_{2,\boldsymbol{k}+\boldsymbol{Q}})^2 + \frac{1}{4}\left(\xi_{1,\boldsymbol{k}}^2 - \xi_{2,\boldsymbol{k}+\boldsymbol{Q}}^2\right)^2 + 4\boldsymbol{M}^2|\Delta_t|^2[1 - (\hat{\boldsymbol{M}}\cdot\hat{\boldsymbol{d}})^2]. \quad (20)$$

These results agree with those of Refs. [20,21] for $\Delta_t = 0$. The self-consistent equations for the order parameters can be calculated from the stationary points $\partial f(\boldsymbol{M},\Delta_s,\Delta_t) = 0$ or, alternatively, through $\langle\psi_{\boldsymbol{k}}\psi_{\boldsymbol{k}}^\dagger\rangle = -T\sum_{\omega_n}\hat{\mathcal{G}}_{\boldsymbol{k},i\omega_n}$. The matrix inversion of $\hat{\mathcal{G}}_k^{-1}$ is straightforward. For instance, the triplet SC OP is given by

$$\Delta_t = -V_t\int_k \frac{\mathcal{Q}_M\boldsymbol{M}\cdot\hat{\boldsymbol{d}} + \mathcal{Q}_d}{\left(\omega_n^2 + E_{+,\boldsymbol{k}}^2\right)\left(\omega_n^2 + E_{-,\boldsymbol{k}}^2\right)}, \quad (21)$$

where $\mathcal{Q}_M = \Delta_s(\xi_{1,\boldsymbol{k}} + \xi_{2,\boldsymbol{k}+\boldsymbol{Q}}) - 2\Delta_t\boldsymbol{M}\cdot\hat{\boldsymbol{d}}$ and $\mathcal{Q}_d = \Delta_t(\boldsymbol{M}^2 - |\Delta_t|^2 - \omega_n^2 - \xi_{1,\boldsymbol{k}}\xi_{2,\boldsymbol{k}+\boldsymbol{Q}}) + \Delta_t^*\Delta_s^2$. It is straightforward to show that, in general, t-SC order does not spontaneously appear (see also Ref. [48]). For instance, in the equation above, setting $M = \Delta_s = 0$ and assuming perfect nesting yields the following linearized equation for Δ_t:

$$\Delta_t = (V_t\rho_F)\Delta_t T_{c,t}\sum_n\int d\xi\,\frac{\omega_n^2 - \xi^2}{\left(\omega_n^2 + \xi^2\right)^2},$$
$$T_{c,t} = \frac{W}{2\,\mathrm{arctanh}\left(\frac{1}{V_t\rho_F}\right)} \quad (22)$$

where ρ_F is the density of states and $2W$ is the bandwidth. Clearly, $T_{c,t}$ only exists if the triplet pairing interaction V_t is very large, $V_t > \rho_F^{-1}$, implying that the system by itself would never develop t-SC on its own. However, Eq. (21) above shows that, as long as the perfect nesting condition $\xi_{1,\boldsymbol{k}} \neq -\xi_{2,\boldsymbol{k}+\boldsymbol{Q}}$ is not satisfied (a result previously highlighted in Ref. [43]), even if we start with $\Delta_t = 0$, the triplet components $\langle c_{\boldsymbol{k},s}f_{-\boldsymbol{k}-\boldsymbol{Q},s'}\rangle \propto |\boldsymbol{M}|\mathcal{Q}_M \propto |\boldsymbol{M}|\Delta_s$ are self-consistently generated when both $\boldsymbol{M}$ and Δ_s are nonzero. Thus, when the SO(3) symmetry is spontaneously broken and the system undergoes a SC phase transition, the SC state is a combination of singlet and triplet states, even if $V_t = 0$. Similar results were previously obtained in Ref. [37].

Near the tetracritical point, both AFM and SC order parameters are small, and a GL functional approach is justified. In this case, we expand f [Eq. (18)] for small $|\boldsymbol{M}|$, $|\Delta_s|$, and $|\Delta_t|$ and obtain

$$\Delta f \approx \frac{a_m}{2}\boldsymbol{M}^2 + \frac{a_s}{2}|\Delta_s|^2 + \frac{a_t}{2}|\Delta_t|^2 + \lambda\cos\alpha_{st}|\Delta_s||\Delta_t|\boldsymbol{M}\cdot\hat{\boldsymbol{d}} + \frac{u_m}{4}\boldsymbol{M}^4 + \frac{u_s}{4}|\Delta_s|^4 + \frac{u_t}{4}|\Delta_t|^4 + \frac{\gamma_{ms}}{2}\boldsymbol{M}^2|\Delta_s|^2 + \frac{\gamma_{mt} + 2\gamma_{12}[1 - (\hat{\boldsymbol{M}}\cdot\hat{\boldsymbol{d}})^2]}{2}\boldsymbol{M}^2|\Delta_t|^2 + \frac{\gamma_{st} - 2\gamma_{12}\sin^2\alpha_{st}}{2}|\Delta_s|^2|\Delta_t|^2, \quad (23)$$

where $\Delta f = f - f(0,0,0)$. The microscopic expressions for the GL coefficients in terms of the dispersions $\xi_{1,\boldsymbol{k}}$ and $\xi_{2,\boldsymbol{k}+\boldsymbol{Q}}$ and the couplings V_m, V_s, and V_t are listed in Appendix A. Such an expression, without the triplet components, was previously derived for the two-band model in Ref. [21].

III. MEAN-FIELD PHASE DIAGRAM AND COLLECTIVE MODES

A. Mean-field analysis of the Ginzburg-Landau functional

Having derived the GL free energy, Eq. (23), our main goal is to investigate the impact of the t-SC term on the system's behavior. An obvious consequence of the trilinear term coupling Δ_t, M, and Δ_s is the aforementioned appearance of t-SC order as soon as antiferromagnetism and singlet superconductivity coexist, despite the fact that a_t remains positive for all temperatures (i.e., there is no spontaneous t-SC order). More specifically, minimization of the GL functional leads to $|\Delta_t| \propto |\boldsymbol{M}||\Delta_s|$. Thus, because Δ_t is naturally of second order in M and Δ_s, we can safely neglect the term $|\Delta_t|^4 \propto |\boldsymbol{M}|^4|\Delta_s|^4$ in the free-energy density, as it is effectively of eighth order.

We proceed by establishing the phase diagram for the AFM, SC, and t-SC orders within mean field. First, without loss of generality, we use $\boldsymbol{M}$ to define a spherical coordinate system in which $\hat{e}_\rho$ is parallel to $\boldsymbol{M}$, so that $\boldsymbol{M} = M\hat{e}_\rho$ and the other unit vectors are defined in the usual way, as shown in Fig. 1. We then decompose $\hat{\boldsymbol{d}}$ as $\hat{\boldsymbol{d}} = d_\rho\hat{e}_\rho + d_\theta\hat{e}_\theta + d_\varphi\hat{e}_\varphi$. The angle between $\boldsymbol{M}$ and $\hat{\boldsymbol{d}}$ is denoted α_{md}, i.e., $\hat{e}_\rho\cdot\hat{\boldsymbol{d}} = d_\rho = \cos\alpha_{md}$. Finally, we define β as the angle between the projection of $\hat{\boldsymbol{d}}$ onto the plane defined by $(\hat{e}_\theta,\hat{e}_\varphi)$ and the direction of $\hat{e}_\theta$, so that $d_\theta = \sin\alpha_{md}\cos\beta$ and $d_\varphi = \sin\alpha_{md}\sin\beta$ (see Fig. 1).

It is useful to introduce a nine-dimensional "supervector" that contains all the OPs, corresponding to the amplitude and phase of each of the two SC order parameters, the two angles characterizing the unit d-vector, and the three

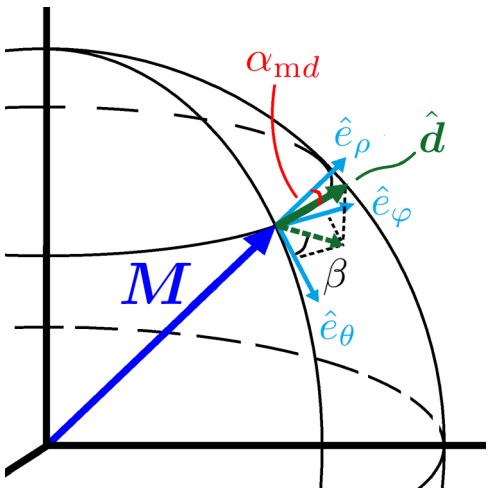

FIG. 1. Schematics of the staggered magnetization $\boldsymbol{M}$ and the triplet unit vector $\hat{\boldsymbol{d}}$. We choose a spherical coordinate system with the ρ vector along $\boldsymbol{M}$, i.e., $\boldsymbol{M} = M\hat{e}_\rho$, and define the angle between the staggered magnetization and the d-vector as α_{md}. The free-energy density does not depend on the angle β; it only depends on $\hat{\boldsymbol{M}}\cdot\hat{\boldsymbol{d}} = \cos\alpha_{md}$. Therefore, f is invariant with respect to rotations of the d-vector around the staggered magnetization vector $\boldsymbol{M}$.

components of the magnetization. In our coordinate system, $\phi^T = [M_\rho, |\Delta_s|, |\Delta_t|, \alpha_{st}, \alpha_{md}, M_\theta, M_\varphi, \alpha_s, \beta]$. We also define the Hessian matrix $\mathbb{H}_{i,j} = \frac{\partial^2 F}{\partial\phi^i \partial\phi^j}$ and write the free-energy density close to its extremum as

$$\Delta f[\phi^i] = \Delta f[\phi_0^i] + \tfrac{1}{2}\delta\phi^T(\mathbb{H})_{\{\phi_0^i\}}\delta\phi, \tag{24}$$

where $\phi_0^T = [M_{\rho 0}, \ldots, \beta_0]$ is the set of variables at which the first derivatives vanish, i.e., $(\partial_{\phi^i} f)_{\{\phi_0^j\}} = 0$. At the local minimum the Hessian matrix must be positive definite.

The first derivatives of Eq. (23) with respect to the angles α_{st} and α_{md} are given by

$$\frac{\partial f}{\partial \alpha_{st}} = -\sin\alpha_{st}|\Delta_s||\Delta_t|(\lambda M\cos\alpha_{md} + 2\gamma_{12}|\Delta_s||\Delta_t|\cos\alpha_{st}) \tag{25}$$

and

$$\frac{\partial f}{\partial \alpha_{md}} = -\sin\alpha_{md} M|\Delta_t|(\lambda|\Delta_s|\cos\alpha_{st} - 2\gamma_{12}M|\Delta_t|\cos\alpha_{md}), \tag{26}$$

respectively. Clearly, a possible solution is $\sin\alpha_{st} = \sin\alpha_{md} = 0$, which is accomplished by $\alpha_{md\,0} = \alpha_{st\,0} = 0$ or $\alpha_{md\,0} = \alpha_{st\,0} = \pi$. However, these solutions do not correspond to a local minimum of the free energy because, in these cases, since $\lambda > 0$, both $\frac{\partial^2 f}{\partial\alpha_{st\,0}^2}$ and $\frac{\partial^2 f}{\partial\alpha_{md\,0}^2}$ are eigenvalues of the Hessian matrix and negative. The other options are $\alpha_{md\,0} = 0$ and $\alpha_{st\,0} = \pi$ or $\alpha_{md\,0} = \pi$ and $\alpha_{st\,0} = 0$. In these cases, $\partial_{|\Delta_{t0}|} f = 0$ gives

$$|\Delta_{t0}| = \frac{\lambda M_0|\Delta_{s0}|}{a_t + \gamma_{st}|\Delta_{s0}|^2 + \gamma_{mt}M_0^2}. \tag{27}$$

Imposing now $\partial_{M_0} f = 0$ and $\partial_{|\Delta_{s0}|} f = 0$ and plugging the expression above into the resulting equations leads to three different solutions with $M_0 \neq 0$ and/or $|\Delta_{s0}| \neq 0$: (i) a pure singlet SC phase with $|\Delta_{s0}|^2 = -a_s/u_s$, $M_0 = 0$, and $\Delta_{t0} = 0$—the free-energy density for this solution is $f_s = -a_s^2/4u_s$; (ii) a pure AFM phase with $M_0^2 = -a_m/u_m$, $\Delta_{s0} = 0$, and $\Delta_{t0} = 0$, the condensation energy density of which is given by $f_m = -a_m^2/4u_m$; and (iii) coexistence of antiferromagnetism and superconductivity where

$$a_m + u_m M_0^2 + \left(\gamma_{ms} - \frac{\lambda^2}{a_t + \gamma_{st}|\Delta_{s0}|^2 + \gamma_{mt}M_0^2}\right)|\Delta_{s0}|^2 + \frac{\gamma_{mt}\lambda^2 M_0^2|\Delta_{s0}|^2}{\left(a_t + \gamma_{st}|\Delta_{s0}|^2 + \gamma_{mt}M_0^2\right)^2} = 0 \tag{28}$$

and

$$a_s + u_s|\Delta_{s0}|^2 + \left(\gamma_{ms} - \frac{\lambda^2}{a_t + \gamma_{st}|\Delta_{s0}|^2 + \gamma_{mt}M_0^2}\right)M_0^2 + \frac{\gamma_{st}\lambda^2 M_0^2|\Delta_{s0}|^2}{\left(a_t + \gamma_{st}|\Delta_{s0}|^2 + \gamma_{mt}M_0^2\right)^2} = 0. \tag{29}$$

The solution to these equations and the corresponding free-energy density f_{coex} can be obtained numerically.

In addition to the solution $\sin\alpha_{st\,0} = \sin\alpha_{md\,0} = 0$ for Eqs. (25) and (26), the conditions $\partial_{\alpha_{st\,0}} f = 0$ and $\partial_{\alpha_{md\,0}} f = 0$ can also be satisfied when

$$2\gamma_{12}|\Delta_{s0}||\Delta_{t0}|\cos\alpha_{st\,0} = -\lambda M_0\cos\alpha_{md\,0} \tag{30}$$

and

$$2\gamma_{12}M_0|\Delta_{t0}|\cos\alpha_{md\,0} = \lambda|\Delta_{s0}|\cos\alpha_{st\,0}. \tag{31}$$

For the two-band model and the microscopic parameters we are considering (see below), however, we show in Appendix B that only $\sin\alpha_{st\,0} = \sin\alpha_{md\,0} = 0$ is a physical solution corresponding to a minimum of f. It follows that the staggered magnetization $\boldsymbol{M}$ is always parallel or antiparallel to the d-vector and the relative phase α_{st} between the singlet and triplet SC order parameters is either zero or π.

This is as far as we can go phenomenologically. In our case, however, the GL parameters are derived directly from the microscopic band dispersions and interactions, as discussed in Appendix A. These microscopic parameters are set in the following way: momenta are measured in units of k_F and the Fermi energy $\xi_F \equiv k_F^2/2m = \varepsilon_{1,0} - \mu$ is chosen to be $\xi_F = 100\,\text{meV}$, which gives $m = 0.005\,\text{meV}^{-1}$. For the interactions, we used $V_s = 266\,\text{meV}$, so that the mean-field SC transition temperature *in the absence of magnetic order* $T_{c,0} = 1\,\text{meV}$ ($\sim$12 K), and $V_t \approx 0.1V_s$ (so that $a_t = 0.2\,\text{meV}^{-1}$). We also set $V_m = 311\,\text{meV}$ so that the magnetic ordering temperature *at perfect nesting and in the absence of SC* $\bar{T}_{N,0} = 2T_{c,0}$. With these parameters fixed, only two-band parameters are left: $\delta_0(k)$, which describes the difference between the areas of hole and electron pockets, and $\delta_2(k)$, which describes the ellipticity of the electron Fermi pocket. Following previous works [20,21], we consider the limit of small Fermi pockets and evaluate these quantities at k_F, i.e., $\delta_0 \equiv \delta_0(k_F)$ and $\delta_2 \equiv \delta_2(k_F)$. For a fixed value of δ_2, we vary δ_0 to mimic the effect of doping and obtain the phase diagram by calculating the instability lines of each of the three GL solutions discussed above and comparing their free energies f_s, f_m, and f_{coex}. In all cases considered, we noted that the GL parameters u_s, λ, $\gamma_{st} = 2\gamma_{12}$, and γ_{ms} are positive, whereas γ_{mt} is negative. The parameter λ, on the other hand, is such that $\text{sign}(\lambda) = \text{sign}(\delta_0)$. We will consider only the regime $u_m > 0$ because this results in a second-order AFM phase transition. If $u_m < 0$, we need to expand the free energy to at least sixth order and, in this case, if the sixth-order coefficient is positive the transition will be first order. More details about the GL coefficients can be found in Appendix A.

The phase diagram of the system in the (T, δ_0) plane is shown in Fig. 2 for a fixed value of δ_2. Besides the purely AFM and singlet SC phases, there is also the coexistence phase where both AFM and singlet SC are present, and hence a triplet SC component is present as well. This coexistence of SC and AFM is microscopic, since the U(1) and SO(3) symmetries are simultaneously broken at each and every unit cell of the lattice. In other words, the lines bounding the AFM-SC region in Fig. 2 are true continuous phase transition lines terminating at a tetracritical point, and not spinodal lines related to a bicritical point.

A similar phase diagram, but without the inclusion of triplet SC, was obtained directly from the microscopic theory in Ref. [20]. What is the net effect of the t-SC contribution? It turns out that the AFM-SC coexistence phase *expands* when

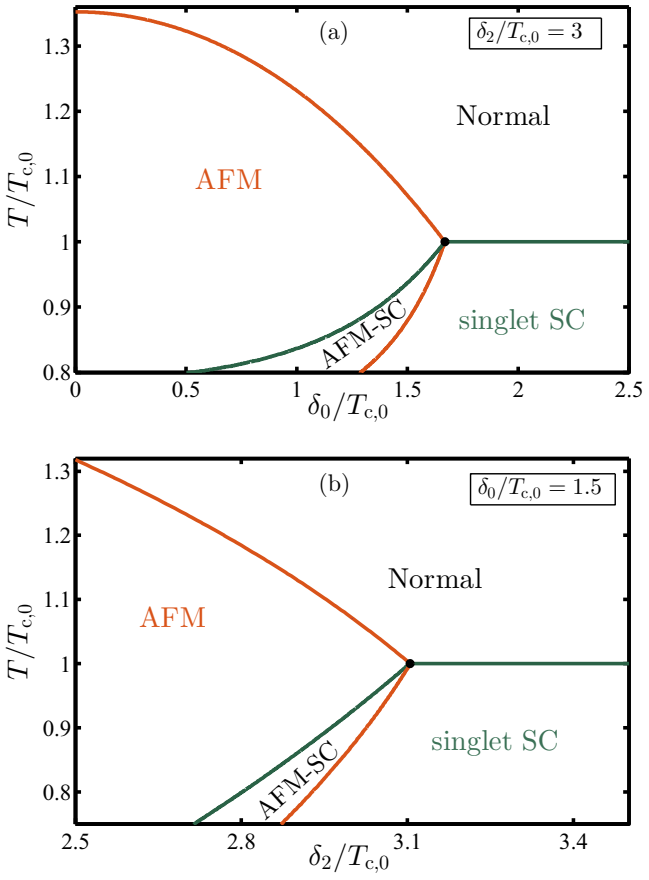

FIG. 2. Phase diagram in the (a) (T,δ_0) and (b) (T,δ_2) planes. The green (orange) curve is the singlet SC (AFM) critical temperature. M_0 and Δ_{s0} are both nonzero in the coexistence region located between the green and the orange curves. Therefore, in this region, $|\Delta_{t0}| \propto M_0|\Delta_{s0}|$ is also nonzero. The black dots denote the tetracritical points. Their coordinates are (a) $(\delta_0^*, T^*) = (1.669, 1)T_{c,0}$ and (b) $(\delta_2^*, T^*) = (3.105, 1)T_{c,0}$.

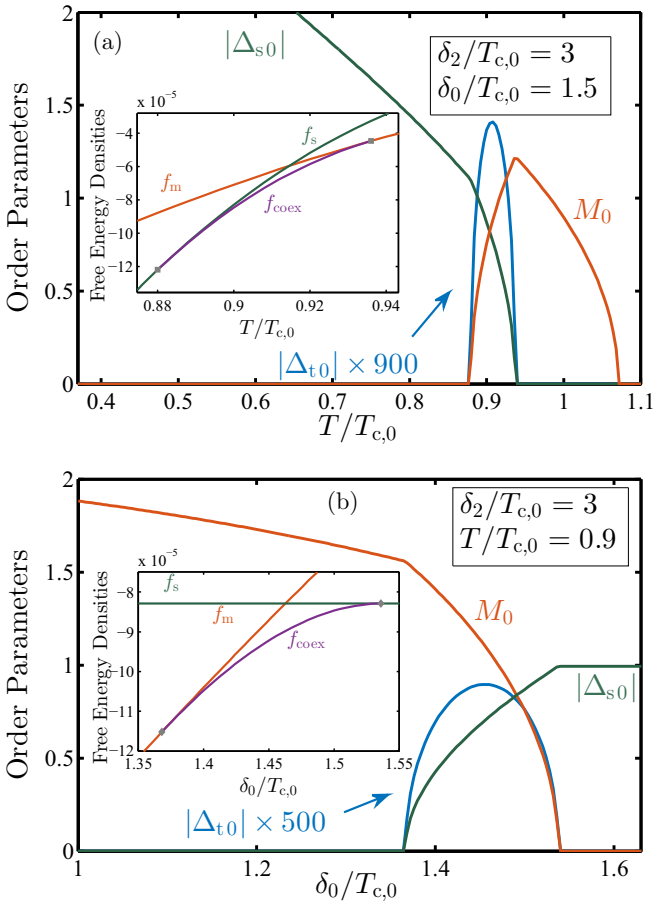

FIG. 3. The behaviors of the singlet SC, triplet SC, and AFM order parameters (Δ_{s0}, Δ_{t0}, and M_0, respectively) as a function of temperature T [(a) fixed δ_0] and δ_0 [(b) fixed temperature] in the phase diagram of Fig. 2. The condensation energies of the pure SC phase f_s, of the pure magnetic phase f_m, and of the AFM-SC coexistence phase f_{coex} are shown in the insets. In order to show all quantities in the same plots, we multiplied Δ_{t0} by multiplicative factors, as indicated in the figure.

compared to the case without triplet SC. This stabilizing effect of the triplet pairing can be understood in simple terms. The smallness of Δ_t allows us to safely neglect the effectively sixth-order terms $|\Delta_t|^2|\Delta_s|^2 \propto |\boldsymbol{M}|^2|\Delta_s|^4$ and $|\Delta_t|^2|\boldsymbol{M}|^2 \propto |\boldsymbol{M}|^4|\Delta_s|^2$ in Eq. (23). In this case, Eq. (27) becomes $|\Delta_{t0}| = \lambda M_0|\Delta_{s0}|/a_t$. Eliminating this variable from the free-energy density, we obtain a simplified expression in terms of the AFM and singlet SC OPs only:

$$\Delta f_{ms} \approx \frac{a_m}{2}\boldsymbol{M}^2 + \frac{a_s}{2}|\Delta_s|^2 + \frac{u_m}{4}\boldsymbol{M}^4 + \frac{u_s}{4}|\Delta_s|^4 + \frac{\gamma_{eff}}{2}\boldsymbol{M}^2|\Delta_s|^2, \quad (32)$$

where the effective quartic coupling between $\boldsymbol{M}^2$ and $|\Delta_s|^2$ is given by

$$\gamma_{eff} = \gamma_{ms} - \lambda^2/a_t. \quad (33)$$

Thus, we note that the competition between singlet SC and AFM is alleviated due to the coupling with the t-SC state, as $\gamma_{eff} < \gamma_{ms}$, i.e., the triplet degrees of freedom promote an *effective attraction* between the AFM and SC order parameters. Evidently, this causes no changes in the pure singlet SC and AFM solutions.

In Fig. 3, we show explicitly the behavior of the three order parameter, Δ_s, Δ_t, and M, as functions of temperature (for fixed $\delta_0/T_{c,0} = 1.5$) and as functions of δ_0 (for fixed temperature $T/T_{c,0} = 0.9$). The competition between Δ_s and M is evident, as well as the secondary character of the triplet order parameter, which is much smaller than Δ_s and M. Indeed, note that, for the reasonably realistic model parameters we used, $|\Delta_{t0}|/|\Delta_{s0}| = \lambda M_0/a_t \approx 10^{-3} M_0/T_{c,0} \approx 10^{-3}$. The condensation energies of each phase are also shown in the insets, highlighting that the AMF-SC coexistence region is indeed the global energy minimum.

B. Excitations in the AFM-SC coexistence state

Having shown that the phase diagram contains the AFM-SC coexistence phase, we now discuss its collective modes by studying the Hessian matrix $\mathbb{H}_{i,j}$ defined in Eq. (24). Inspection of Eq. (23) reveals that the free energy is independent

of the last four components of the supervector ϕ. Therefore, the corresponding 4×4 block of $\mathbb{H}_{i,j}$ vanishes identically. Evidently, this reflects (a) the rotational SO(3) symmetry of the antiferromagnetic order parameter (M_θ, M_φ), (b) the global U(1) symmetry of the SC order parameter (α_s), and (c) the fact that the vector $\hat{\boldsymbol{d}}$ can be freely rotated around the antiferromagnetic order parameter without any energy cost (β). These symmetries are spontaneously broken in the ordered phases. There is one Goldstone mode associated with each one of these variables once the corresponding symmetries are broken, except for the global SC phase α_s which is gapped out by the coupling to the electromagnetic field through the Anderson-Higgs mechanism. We will drop this 4×4 block in what follows, and focus on the nonvanishing part of the Hessian matrix in the coexistence state, given by

$$\mathbb{H} = \left[\begin{array}{c|cc} \mathbb{C}_{3\times 3} & 0 & 0 \\ \hline 0 & \frac{\partial^2 f}{\partial \alpha_{\rm st}^2} & 0 \\ 0 & 0 & \frac{\partial^2 f}{\partial \alpha_{{\rm m}d}^2} \end{array}\right], \tag{34}$$

where

$$\frac{\partial^2 f}{\partial \alpha_{\rm st}^2} = \frac{\lambda^2 M^2 \Delta_{\rm s}^2}{a_{\rm t} + \gamma_{\rm st}\Delta_{\rm s}^2 + \gamma_{\rm mt} M^2}\left(1 - \frac{2\gamma_{12}\Delta_{\rm s}^2}{a_{\rm t} + \gamma_{\rm st}\Delta_{\rm s}^2 + \gamma_{\rm mt} M^2}\right) \tag{35}$$

and

$$\frac{\partial^2 f}{\partial \alpha_{{\rm m}d}^2} = \frac{\lambda^2 M^2 \Delta_{\rm s}^2}{a_{\rm t} + \gamma_{\rm st}\Delta_{\rm s}^2 + \gamma_{\rm mt} M^2}\left(1 + \frac{2\gamma_{12} M^2}{a_{\rm t} + \gamma_{\rm st}\Delta_{\rm s}^2 + \gamma_{\rm mt} M^2}\right). \tag{36}$$

While the 3×3 matrix $\mathbb{C}_{3\times 3}$ refers to collective amplitude modes related to the equilibrium values of $\Delta_{\rm s}$, $\Delta_{\rm t}$, and M, the last two quantities refer to the relative phase between the two SC order parameters, $\alpha_{\rm st}$, and to the relative angle between the d-vector and the magnetization, $\alpha_{{\rm m}d}$. Although $\mathbb{C}_{3\times 3}$ is straightforward to obtain, we refrain from writing out explicitly its lengthy expression here. We have scanned exhaustively the values of δ_0, δ_2, and T in the AFM-SC coexistence region and found consistently that the eigenvalues of $\mathbb{C}_{3\times 3}$ are indeed always positive, which proves that we have a locally stable phase. Moreover, as emphasized before, it is also the global minimum.

As for the terms $\frac{\partial^2 f}{\partial \alpha_{\rm st}^2}$ and $\frac{\partial^2 f}{\partial \alpha_{{\rm m}d}^2}$, we also found them to be always positive. Specifically, Eq. (35) gives the "mass" (i.e., the energy at $\boldsymbol{k}=0$) of the collective mode associated with oscillations of the relative phase between the two SC order parameters. It is thus the analog of the Leggett mode of two-band SCs [53]. Similarly, the other second derivative in Eq. (36) gives the "mass" of another collective mode corresponding to oscillations of the angle between the AFM OP and the $\hat{\boldsymbol{d}}$ vector of the t-SC OP. It is useful to consider the simplified GL functional in Eq. (32), which was obtained after neglecting the effectively sixth-order terms coming from the t-SC OP. In this approximation we find

$$\frac{\partial^2 f}{\partial \alpha_{{\rm st}\,0}^2} = \frac{\partial^2 f}{\partial \alpha_{{\rm m}d\,0}^2} = \frac{\lambda^2}{a_{\rm t}} M_0^2 \Delta_{{\rm s}\,0}^2. \tag{37}$$

Thus, the masses of the Leggett mode and of the angular mode between $\boldsymbol{M}$ and $\hat{\boldsymbol{d}}$ become degenerate. As we have seen above, this degeneracy is lifted with the inclusion of the sixth-order terms.

IV. IMPACT OF FLUCTUATIONS ON THE PHASE DIAGRAM

In this section we go beyond the previous mean-field analysis and investigate the impact of Gaussian fluctuations on the phase diagram of Fig. 2. Because the SC transition is usually well described by a mean-field transition, we here focus on the impact of magnetic fluctuations only. In particular, our goal is to determine how the mean-field critical temperatures ($T_{\rm c,0}$ and $T_{\rm N,0}$) as well as the coexistence region are affected by these magnetic fluctuations.

We first generalize the uniform staggered magnetization to an inhomogeneous function of space $\boldsymbol{M} \to \boldsymbol{M}_{\boldsymbol{x}}$, or in the Fourier space $\boldsymbol{M}_{\boldsymbol{q}} = \sum_{\boldsymbol{x}} e^{i\boldsymbol{q}\cdot\boldsymbol{x}} \boldsymbol{M}_{\boldsymbol{x}}$. We assume this extension does not change in a relevant way any coupling other than the quadratic magnetic coefficient of the free energy [Eq. (23)], whereby $\frac{a_{\rm m}}{2}\boldsymbol{M}^2 \to \frac{a_{\rm m}+g_{\boldsymbol{q}}}{2}|\boldsymbol{M}_{\boldsymbol{q}}|^2$, where $(a_{\rm m}+g_{\boldsymbol{q}})^{-1}$ is the momentum-dependent magnetic susceptibility with $g_{\boldsymbol{q}}$ being some function of momentum such that $g_0 = 0$.

We decouple the quartic AFM term in the partition function, $Z \propto \int \mathcal{D}[\boldsymbol{M}, \Delta_{\rm s}, \Delta_{\rm t}] e^{-F/T}$, via a Hubbard-Stratonovitch transformation [54]:

$$e^{-\frac{u_{\rm m}}{4T}\sum_{\boldsymbol{x}} \boldsymbol{M}_{\boldsymbol{x}}^4} \propto \int \mathcal{D}[\psi] e^{-\frac{1}{2T}\sum_{\boldsymbol{x}}(-\frac{\psi_{\boldsymbol{x}}^2}{2u_{\rm m}} + \boldsymbol{M}_{\boldsymbol{x}}^2\psi_{\boldsymbol{x}})}. \tag{38}$$

The price we pay when we introduce the auxiliary Hubbard-Stratonovitch field is an additional degree of freedom in the partition function ($\mathcal{D}[\psi]$). The effective free-energy density thus becomes quadratic in the magnetic order parameter

$$\begin{aligned} f_{\rm eff} = {} & \frac{a_{\rm s}}{2}|\Delta_{\rm s}|^2 + \frac{a_{\rm t}}{2}|\Delta_{\rm t}|^2 + \frac{u_{\rm s}}{4}|\Delta_{\rm s}|^4 - \frac{\psi^2}{4u_{\rm m}} \\ & + \frac{1}{2\upsilon^2}\sum_{\boldsymbol{q}}(g_{\boldsymbol{q}} + a_{\rm m} + \gamma_{\rm ms}|\Delta_{\rm s}|^2 + \psi)|\boldsymbol{M}_{\boldsymbol{q}}|^2 \\ & + \frac{1}{\upsilon^2}\sum_{\boldsymbol{q}} \lambda\cos\alpha_{\rm st}|\Delta_{\rm s}||\Delta_{\rm t}|\boldsymbol{M}_{\boldsymbol{q}}\cdot\boldsymbol{d}_{-\boldsymbol{q}}, \end{aligned} \tag{39}$$

where $\hat{\boldsymbol{d}}_{\boldsymbol{q}} = \sum_{\boldsymbol{x}} e^{i\boldsymbol{q}\cdot\boldsymbol{x}}\hat{\boldsymbol{d}} = \upsilon\delta_{\boldsymbol{q},0}\hat{\boldsymbol{d}}$ and we have neglected the sixth and higher order terms $|\Delta_{\rm t}|^4$, $|\Delta_{\rm t}|^2|\Delta_{\rm s}|^2$, and $|\Delta_{\rm t}|^2|\boldsymbol{M}_{\boldsymbol{q}}|^2$. Note that we assumed $\psi_{\boldsymbol{x}}$ to be homogeneous, which can be justified in the saddle-point approximation that corresponds to evaluating the partition function at $\partial f_{\rm eff}(\psi)/\partial\psi = 0$. At this saddle point, $\psi = u_m\langle M^2\rangle$ is proportional to the Gaussian magnetic fluctuations. The saddle point can be justified in an appropriate large-N limit of a theory in which the number of components of $\boldsymbol{M}$ is enlarged from $3 \to N$. The integration over the $\Delta_{\rm t}$ fields can always be done, in any state, because according to Eq. (22) the field is always massive, i.e., $a_{\rm t} > 0$ at all temperatures. Then, we introduce $\Delta_{\rm t}\boldsymbol{d} = \boldsymbol{\Delta}_{\rm t}$ and integrate over $\Delta_{{\rm t},j}$ to obtain

$$\begin{aligned} f_{\rm eff} = {} & \frac{a_{\rm s}}{2}|\Delta_{\rm s}|^2 + \frac{u_{\rm s}}{4}|\Delta_{\rm s}|^4 - \frac{\psi^2}{4u_{\rm m}} \\ & + \frac{1}{2\upsilon^2}\sum_{\boldsymbol{q}}(g_{\boldsymbol{q}} + a_{\rm m} + \gamma_{\rm eff}|\Delta_{\rm s}|^2 + \psi)|\boldsymbol{M}_{\boldsymbol{q}}|^2, \end{aligned} \tag{40}$$

where $\gamma_{\rm eff}$ was defined in Eq. (33).

We also introduce magnetic long-range order by allowing the radial component of $\boldsymbol{M_q}$ to have a nonzero mean value. We write $M_{\boldsymbol{q}}^{(\rho)} \to \upsilon M \delta_{\boldsymbol{q},0} + (1-\delta_{\boldsymbol{q},0}) M_{\boldsymbol{q}}^{(\rho)}$ and integrate out the magnetic fluctuations $M_{\boldsymbol{q}}^{(j)}$ to obtain

$$f_{\text{eff}} = \frac{a_s}{2}|\Delta_s|^2 + \frac{u_s}{4}|\Delta_s|^4 - \frac{\psi^2}{4u_m} + \frac{r}{2}M^2 + \frac{NT}{2\upsilon}\sum_{\boldsymbol{q}} \ln(g_{\boldsymbol{q}} + r) - \frac{T}{2\upsilon}\ln r, \tag{41}$$

where $r = a_m + \gamma_{\text{eff}}|\Delta_s|^2 + \psi$ is the "mass" of the fully renormalized susceptibility. In order to extended the number of components of the staggered magnetization from $N = 3$ to arbitrary N we have to rescale the OP and the couplings as $(M^2, \Delta_s^2) \to (M^2, \Delta_s^2)N$ and $(u_s, u_m, \gamma_{\text{eff}}) \to (u_s, u_m, \gamma_{\text{eff}})/N$. The effective free-energy density then reads

$$f_{\text{eff}}/N = \frac{a_s}{2}|\Delta_s|^2 + \frac{u_s}{4}|\Delta_s|^4 - \frac{\psi^2}{4u_m} + \frac{r}{2}M^2 + \frac{T_{c,0}}{2\upsilon}\sum_{\boldsymbol{q}} \ln(g_{\boldsymbol{q}} + r), \tag{42}$$

for $N \gg 1$. In the spirit of the GL approximation we have set $T \approx T_{c,0}$ in the last term of the above equation.

Extremizing f_{eff} with respect to the Hubbard-Stratonovitch field ψ leads to the following equation:

$$\frac{\psi}{u_m} = M^2 + \mathcal{I}(r), \tag{43}$$

where

$$\mathcal{I}(r) = \frac{T_{c,0}}{\upsilon}\sum_{\boldsymbol{q}} \frac{1}{g_{\boldsymbol{q}} + r}. \tag{44}$$

On the other hand, extremizing f_{eff} with respect to the order parameters M and $|\Delta_s|$ we obtain

$$M = 0 \quad \text{or} \quad r = 0 \tag{45}$$

and

$$|\Delta_s| = 0 \quad \text{or} \quad a_s + u_s|\Delta_s|^2 + \frac{\gamma_{\text{eff}}\psi}{u_m} = 0, \tag{46}$$

respectively. The set of Eqs. (43)–(46) has four different solutions, as in the case without magnetic fluctuations. The possible phases are (i) a pure singlet SC phase with $M = 0$, $\psi = u_m\mathcal{I}(a_m + \gamma_{\text{eff}}|\Delta_s|^2 + \psi)$, and

$$|\Delta_s|^2 = -\frac{a_s}{u_s} - \frac{\gamma_{\text{eff}}\psi}{u_s u_m}; \tag{47}$$

(ii) a pure AFM phase with $\Delta_s = 0$, $\psi = -a_m$, and

$$M^2 = -\frac{a_m}{u_m} - \mathcal{I}(0); \tag{48}$$

(iii) a phase of coexistence of AFM and SC with $r = 0$,

$$|\Delta_s|^2 = \frac{a_m\gamma_{\text{eff}} - a_s u_m}{u_s u_m - \gamma_{\text{eff}}^2}, \tag{49}$$

and

$$M^2 = \frac{a_s\gamma_{\text{eff}} - a_m u_s}{u_s u_m - \gamma_{\text{eff}}^2} - \mathcal{I}(0); \tag{50}$$

and (iv) the normal state with $\Delta_s = M = 0$ and $r - a_m = u_m\mathcal{I}(r)$.

The quantity $\mathcal{I}(0)$ in Eq. (48) measures the change in the AFM critical temperature $T_{N,0}$ due to the Gaussian AFM fluctuations. Since $\mathcal{I}(r) \geqslant 0$, we conclude that $T_{N,0}$ is suppressed by magnetic fluctuations, as expected. We can also see from Eq. (44) that, in a two-dimensional system, the magnetic fluctuations correction diverges ($\mathcal{I}(0) \to \infty$), thus destroying the magnetic order. This is a consequence of the Mermin-Wagner theorem [55], which states that a finite-temperature AFM transition only happens for dimensions $d > 2$. We will, therefore, consider an anisotropic three-dimensional model of weakly coupled layers, for which [54]

$$g_{\boldsymbol{q}} = \kappa\left(q_x^2 + q_y^2\right) + \eta_z \sin^2(q_z/2) \tag{51}$$

with $0 \leqslant q_z < 2\pi$ and $\eta_z < \kappa$. A detailed derivation of the microscopic expression for κ can be found in Appendix A. Carrying out the calculations we obtain

$$\mathcal{I}(r) = \frac{T_{c,0}}{2\pi\kappa}\ln\left(\frac{\sqrt{r+\kappa\Lambda^2} + \sqrt{r+\kappa\Lambda^2+\eta_z}}{\sqrt{r} + \sqrt{r+\eta_z}}\right), \tag{52}$$

where Λ is an ultraviolet cutoff [54]. For completeness, we also show the result of the momentum summation in the last term of the effective free energy (42):

$$\begin{aligned}\mathcal{I}_\ell(r) &\equiv \frac{1}{\upsilon}\sum_{\boldsymbol{q}} \ln(g_{\boldsymbol{q}} + r) \\ &= \frac{\Lambda^2}{2\pi}\ln\left(\sqrt{r+\kappa\Lambda^2} + \sqrt{r+\kappa\Lambda^2+\eta_z}\right) \\ &\quad + \frac{\eta_z + 2r}{4\pi\kappa}\ln\left(\frac{\sqrt{r+\kappa\Lambda^2} + \sqrt{r+\kappa\Lambda^2+\eta_z}}{\sqrt{r} + \sqrt{r+\eta_z}}\right) \\ &\quad + \frac{\sqrt{r+\kappa\Lambda^2} - \sqrt{r+\kappa\Lambda^2+\eta_z}}{4\pi\kappa} + \text{const.}\end{aligned} \tag{53}$$

We solved the set of coupled nonlinear equations for r, $|\Delta_s|^2$, and M^2 and compared the values of the free energies of the possible phases to obtain the fluctuation-corrected phase diagram of the model, as shown in Fig. 4(a). We set $\eta_z = 0.3\kappa$ and $\Lambda^2 = k_F^2 = 10$. The shaded areas represent the fluctuation-corrected phases, whereas the full lines represent the phase transition boundaries in the absence of fluctuations [i.e., the same lines depicted in Fig. 2(a)]. We clearly see that both the mean-field SC and the mean-field Néel critical temperatures are reduced by the magnetic fluctuations. These suppressions occur because the last terms of Eqs. (47) and (48) are negative, i.e., the OPs are reduced. Analogously, the effect of the magnetic fluctuations on M^2 in the coexistence phase is given by the last term of Eq. (50), which is negative. We illustrate the effect of the magnetic fluctuations on the staggered magnetization in Fig. 4(b), which shows that the reduction of M within the AFM-SC coexistence region implies that the *lower* temperature at which magnetic order disappears is *enhanced* by the magnetic fluctuations. Finally, the SC transition temperature in the magnetically ordered state occurs at the same temperature when compared to the case without magnetic fluctuations. This is evident from Eq. (49), since the singlet SC OP is not affected by the magnetic fluctuations.

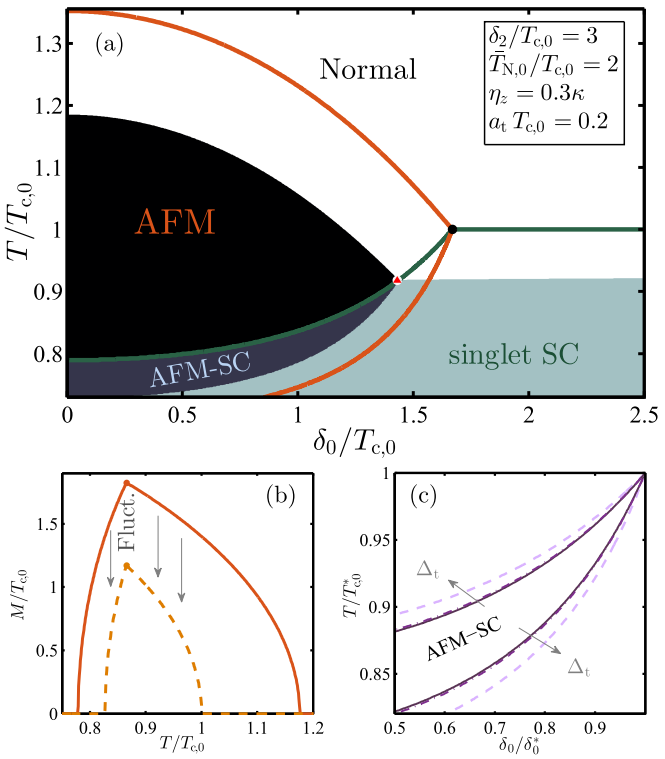

FIG. 4. (a) Fluctuation-corrected phase diagram in the (T,δ_0) plane. The black, light gray, dark gray, and white regions are the pure AFM, pure SC, coexistence AFM-SC, and normal phases, respectively. The green and orange curves represent the phase diagram without fluctuations [same lines as in Fig. 2(a)]. Clearly, magnetic fluctuations shrink the AFM region. The "new" multicritical point, represented by the red triangle, is still a tetracritical point. (b) The AFM order parameter for the same parameters of panel (a) and $\delta_0 = 1.20\, T_{c,0}$ with (dashed line) and without (solid line) the inclusion of magnetic fluctuations. The solid circles denote the positions of the SC critical temperatures. (c) The effect of the triplet SC order parameter on the boundaries of the coexistence region: the greater the value of a_t, the smaller Δ_t becomes. Solid curves are for $a_t \to \infty$ ($\Delta_t \equiv 0$), dash-dotted curves are for $a_t = 0.2\,\text{meV}^{-1}$ [as in panel (a)], and dashed curves are for $a_t = 0.02\,\text{meV}^{-1}$.

In fact, it can be easily shown that, within our treatment, the effective action for Δ_s (after integrating over the other OPs) is the same both with and without the inclusion of Gaussian fluctuations.

To elucidate the role of the triplet degrees of freedom on the coexistence phase, we also changed the value of a_t, since $|\Delta_t| \propto a_t^{-1}$. We show the transition lines to the AFM-SC coexistence phase for three different values of a_t in Fig. 4(c). Clearly, the larger the value of $|\Delta_t|$ the larger the size of the AFM-SC region, thus showing that the stabilizing effect of the triplet component on the coexistence region is not restricted to the mean-field analysis of Sec. III A, but is also present when fluctuations are included. The most prominent result of these renormalizations, therefore, is the evident shrinking of the AFM region caused by the magnetic fluctuations, which is to be expected. We checked, by comparing the various free energies, that the phases indicated in Fig. 4 are indeed the thermodynamically stable phases of the system. Furthermore, all the phase transition lines keep their second-order character and their intersection remains a tetracritical point.

V. CONCLUSIONS

In this paper, we studied the impact of the spin-triplet pairing component on the phase diagram of competing AFM and SC orders. Except in very special cases, such as systems with perfectly nested bands, the t-SC is always present in the AFM-SC coexistence phase, and is therefore an integral part of the phase diagram of systems displaying these two types of order. As we showed, in general the triplet degrees of freedom suppress the competition between AFM and SC by mediating an effective attraction between these otherwise competing orders. More importantly, we investigated in detail the coupling between the triplet d-vector and the staggered magnetization. In the ordered state, this coupling forces the d-vector to align parallel or antiparallel to the AFM order parameter. It also promotes the emergence of two collective modes in the AFM-SC coexistence state. The first one is a Goldstone mode related to the precession of the d-vector around the staggered magnetization. The second one is a massive mode that is nearly degenerate with the Leggett-type mode associated with the relative phase between the singlet and triplet components of the SC order parameter. The experimental detection of these modes would provide unambiguous evidence for a microscopic AFM-SC state, in contrast to the more trivial situation of phase separated domains displaying either AFM or SC order, but not both.

We also went beyond the Ginzburg-Landau mean-field approach and studied the impact of Gaussian magnetic fluctuations on the phase diagram. We found that, as expected, the inclusion of these fluctuations acts mainly to shrink the region where AFM order exists, while at the same time keeping the second-order nature of the phase transition lines and tetracritical character of the multicritical point. Our main result is that, despite the fact that AFM and SC are competing orders, the coupling between magnetic and t-SC degrees of freedom always favors an enhancement of the AFM-SC coexistence state. Although in this paper we considered a particular two-band microscopic model, which has been widely employed in the study of iron-based superconductors, much of our conclusions relies solely on the properties of the Ginzburg-Landau free energy, such as the AFM-singlet SC attraction promoted by the t-SC degrees of freedom, the coupling between the triplet d-vector and the staggered magnetization, and the nature of the collective modes inside the AFM-SC coexistence state. Consequently, we expect these results to be relevant not only for iron pnictides but also for cuprates and heavy fermion materials. Overall, the impact of the t-SC degrees of freedom on the phase diagram of competing AFM and SC states highlights the importance of composite orders arising in the regime where two distinct types of order have comparable energies, illustrating that their interplay goes beyond just the competition for the same electronic states.

ACKNOWLEDGMENTS

We thank D. Agterberg, A. Chubukov, J. Kang, and M. Schuett for useful discussions. D.E.A. was supported by

the agencies CNPq (Brazil) and CAPES (Brazil). R.M.F. is supported by the U.S. Department of Energy, Office of Science, Basic Energy Sciences, under Award No. DE-SC0012336. E.M. is supported by CNPq (Grant No. 304311/2010-3).

APPENDIX A: GINZBURG-LANDAU FUNCTIONAL COEFFICIENTS

The coefficients of the GL expansion of the free-energy density f [Eq. (23)] are given by

$$a_{\rm m} = \frac{4}{V_{\rm m}} + 4\int_k G_{1,k}G_{2,k}, \quad u_{\rm m} = 4\int_k G_{1,k}^2 G_{2,k}^2, \tag{A1}$$

$$a_{\rm s} = \frac{4}{V_{\rm s}} - 2\sum_\alpha \int_k G_{\alpha,k}G_{\alpha,-k}, \quad u_{\rm s} = 2\sum_\alpha \int_k G_{\alpha,k}^2 G_{\alpha,-k}^2, \tag{A2}$$

$$a_{\rm t} = \frac{4}{V_{\rm t}} - 4\int_k G_{1,k}G_{2,-k}, \quad u_{\rm t} = 4\int_k G_{1,k}^2 G_{2,-k}^2, \tag{A3}$$

$$\lambda = -2\sum_\alpha \int_k G_{\alpha,k}G_{\alpha,-k}(G_{\bar\alpha,k} + G_{\bar\alpha,-k}), \tag{A4}$$

$$\gamma_{12} = 4\int_k G_{1,k}G_{1,-k}G_{2,k}G_{2,-k}, \tag{A5}$$

$$\gamma_{\rm ms} = -4\sum_\alpha \int_k G_{\alpha,k}^2 G_{\alpha,-k}G_{\bar\alpha,k} - \gamma_{12}, \tag{A6}$$

$$\gamma_{\rm mt} = -4\sum_\alpha \int_k G_{\alpha,k}^2 G_{\bar\alpha,k}G_{\bar\alpha,-k} - \gamma_{12}, \tag{A7}$$

and

$$\gamma_{\rm st} = 4\sum_\alpha \int_k G_{\alpha,k}^2 G_{\alpha,-k}G_{\bar\alpha,-k} + \gamma_{12}, \tag{A8}$$

where $G_{1,k}^{-1} = i\omega_n - \xi_{1,\boldsymbol{k}}$ and $G_{2,k}^{-1} = i\omega_n - \xi_{2,\boldsymbol{k}+\boldsymbol{Q}}$ are the noninteracting Green's functions for each band. Note that the symmetry $\xi_{2,\boldsymbol{k}+\boldsymbol{Q}} = \xi_{2,\boldsymbol{k}-\boldsymbol{Q}}$ implies that $G_{2,-k}^{-1} = -i\omega_n - \xi_{2,-\boldsymbol{k}+\boldsymbol{Q}} = -i\omega_n - \xi_{2,-\boldsymbol{k}-\boldsymbol{Q}}$.

In order to gain more analytical insight, we have made the following simplifications, following Ref. [20]: $\delta_0(k) \approx \delta_0(k_F) \equiv \delta_0$ and $\delta_2(k) \approx \delta_2(k_{\rm F}) \equiv \delta_2$, so that $\delta_{\boldsymbol{k}} \to \delta_\theta = \delta_0 + \delta_2\cos(2\theta)$. Here, $k_{\rm F}$ is the Fermi wave vector, defined so that $\xi_{1,k_{\rm F}} = 0$ and $k_{\rm F}^2/2m = \varepsilon_{1,0} - \mu \equiv \xi_{\rm F}$. Thus, we can write the dispersions as $\xi_{1,\boldsymbol{k}} = \xi_k = \xi_{\rm F} - \frac{k^2}{2m}$ and $\xi_{2,\boldsymbol{k}+\boldsymbol{Q}} = -\xi_k + 2\delta_\theta$. This allows us to write $\frac{1}{\upsilon}\sum_{\boldsymbol{k}} \to m\int_0^{2\pi}\frac{d\theta}{2\pi}\int_{-\infty}^{\xi_{\rm F}}\frac{d\xi}{2\pi}$; since we consider the case $\xi_F \ll T$, we can generally send $\xi_{\rm F} \to \infty$ in the upper limit of the integral, provided that the integrand does not vanish. Notice that m is proportional to the two-dimensional density of states.

Carrying out the integrations over momentum and frequency we obtain

$$a_{\rm s} = \frac{2m}{\pi}\ln(T/T_{\rm c,0}), \quad u_{\rm s} = \frac{7\zeta(3)m}{4\pi^3T^2}, \tag{A9}$$

where $T_{\rm c,0} = (2\xi_{\rm F}/\pi)e^{\gamma - 2\pi/mV_{\rm s}}$ and $\gamma \approx 0.577$ is the Euler-Mascheroni constant. Note that these couplings do not depend on the parameters δ_0 and δ_2. Furthermore, $a_{\rm t} = 4/V_{\rm t} - 2m/\pi$ and $u_{\rm t} = 0$ (in the limit of $\xi_{\rm F}/T \to \infty$), and

$$a_{\rm m} = \frac{2m}{\pi}\ln(T/\bar T_{\rm N,0}) + \frac{2m}{\pi}\tilde a_{\rm m}(\tilde\delta_0,\tilde\delta_2), \tag{A10}$$

where $\bar T_{\rm N,0} = (2\xi_{\rm F}/\pi)e^{\gamma - 2\pi/mV_{\rm m}}$, $\tilde\delta_{0\,(2)} = \delta_{0\,(2)}/2\pi T$, and

$$\tilde a_{\rm m}(\tilde\delta_0,\tilde\delta_2) = \gamma + \ln 4 + \frac{1}{2}\left\langle \psi^{(0)}\left(\frac{1}{2} + i\tilde\delta_\theta\right) + \psi^{(0)}\left(\frac{1}{2} - i\tilde\delta_\theta\right)\right\rangle_\theta, \tag{A11}$$

where $\tilde\delta_\theta = \delta_\theta/2\pi T$, $\psi^{(0)}(z)$ is the digamma function and the angular brackets denote angular averages $\langle\cdots\rangle_\theta = \int_0^{2\pi}\frac{d\theta}{2\pi}(\cdots)$.

Finally, introducing the dimensionless quantities $\tilde u_{\rm m} = 4\pi^3T^2u_{\rm m}/m$, $\tilde\lambda = \pi^2T\lambda/m$, $\tilde\gamma_{\rm st} = 2\pi^3T^2\gamma_{\rm st}/m$, $\tilde\gamma_{\rm ms} = 4\pi^3T^2\gamma_{\rm ms}/m$, and $\tilde\gamma_{\rm mt} = -2\pi^3T^2\gamma_{\rm mt}/m$ we find

$$\tilde u_{\rm m} = -\frac{1}{4}\left\langle \psi^{(2)}\left(\frac{1}{2} + i\tilde\delta_\theta\right) + \psi^{(2)}\left(\frac{1}{2} - i\tilde\delta_\theta\right)\right\rangle_\theta, \tag{A12}$$

$$\tilde\lambda = \left\langle \frac{\gamma + \ln 4}{\tilde\delta_\theta} + \frac{\psi^{(0)}\left(\frac{1}{2} + i\tilde\delta_\theta\right) + \psi^{(0)}\left(\frac{1}{2} - i\tilde\delta_\theta\right)}{2\tilde\delta_\theta}\right\rangle_\theta, \tag{A13}$$

$$\tilde\gamma_{\rm st} = \left\langle \frac{\gamma + \ln 4}{\tilde\delta_\theta^2} + \frac{\psi^{(0)}\left(\frac{1}{2} + i\tilde\delta_\theta\right) + \psi^{(0)}\left(\frac{1}{2} - i\tilde\delta_\theta\right)}{2\tilde\delta_\theta^2}\right\rangle_\theta, \tag{A14}$$

$$\tilde\gamma_{\rm mt} = \tilde\gamma_{\rm st} - i\left\langle \frac{\psi^{(1)}\left(\frac{1}{2} + i\tilde\delta_\theta\right) - \psi^{(1)}\left(\frac{1}{2} - i\tilde\delta_\theta\right)}{4\tilde\delta_\theta}\right\rangle_\theta, \tag{A15}$$

and $\tilde\gamma_{\rm ms} = \tilde\gamma_{\rm st} - 2\tilde\gamma_{\rm mt}$. Moreover, $\gamma_{\rm st} = 2\gamma_{12} > 0$. In the expressions above, $\psi^{(n)}(z)$ is the polygamma function of order n, defined as $\psi^{(n)}(z) = \frac{d^{n+1}}{dz^{n+1}}\ln[\Gamma(z)]$, where $\Gamma(z)$ is the gamma function. Away from the perfect nesting condition we can only evaluate these angular averages numerically.

When the staggered magnetization is not a homogeneous function of space and (imaginary) time, the quadratic term in $\boldsymbol{M}$ in the GL expansion [Eq. (23)] becomes $\frac{1}{2}\int_q \chi_{\rm m}^{-1}(\boldsymbol{q},\nu_n)M_q^2$, where

$$\chi_{\rm m}^{-1}(\boldsymbol{q},\nu_n) = \frac{4}{V_{\rm m}} + 4\int_k G_{2,k}G_{1,k-q} \tag{A16}$$

is the frequency- and momentum-dependent magnetic susceptibility. In the static limit, $\nu_n = 0$, and for small $\boldsymbol{q} = |\boldsymbol{q}|(\cos\theta_q, \sin\theta_q)$ this quantity naturally has the same anisotropy as the Fermi surface:

$$\chi_{\rm m}^{-1}(|\boldsymbol{q}| \ll 1, \nu_n = 0) \equiv \chi_{\boldsymbol{q}}^{-1} = a_{\rm m} + q^2(\kappa + \kappa_2\cos 2\theta_q), \tag{A17}$$

where

$$\kappa = \frac{1}{64\pi^2T}\left\langle\left(\tilde\delta_\theta - \frac{\xi_{\rm F}}{2\pi T}\right)\left[\psi^{(2)}\left(\frac{1}{2} + i\tilde\delta_\theta\right) + \psi^{(2)}\left(\frac{1}{2} - i\tilde\delta_\theta\right)\right]\right\rangle_\theta \tag{A18}$$

and

$$\kappa_2 = \frac{1}{64\pi^2 T}\left\langle \cos 2\theta \left(\tilde{\delta}_\theta - \frac{\xi_F}{2\pi T}\right)\left[\psi^{(2)}\left(\frac{1}{2}+i\tilde{\delta}_\theta\right) + \psi^{(2)}\left(\frac{1}{2}-i\tilde{\delta}_\theta\right)\right]\right\rangle_\theta + \frac{i}{32\pi^2 T}\left\langle \cos 2\theta \left[\psi^{(1)}\left(\frac{1}{2}+i\tilde{\delta}_\theta\right) - \psi^{(1)}\left(\frac{1}{2}-i\tilde{\delta}_\theta\right)\right]\right\rangle_\theta . \tag{A19}$$

Note that $\kappa_2 = 0$ when $\delta_2 = 0$, i.e., when δ_θ does not depend on the angle θ. For simplicity, we will neglect the anisotropy so that we can write $\chi_q^{-1} = a_m + \kappa q^2$.

APPENDIX B: MINIMIZATION WITH RESPECT TO α_{md} AND α_{st}

In addition to the solutions $\sin\alpha_{st\,0} = \sin\alpha_{md\,0} = 0$, the extremum conditions $\partial_{\alpha_{st\,0}} f = 0$ and $\partial_{\alpha_{md\,0}} f = 0$ in Eqs. (25) and (26) can also be satisfied by Eqs. (30) and (31), respectively. There are, therefore, four combinations that solve Eqs. (25) and (26): (i) $\sin\alpha_{st\,0} = \sin\alpha_{md\,0} = 0$, (ii) Eqs. (30) and (31), (iii) $\sin\alpha_{st\,0} = 0$ and Eq. (31), and (iv) Eq. (30) and $\sin\alpha_{md\,0} = 0$.

Case (i) was studied in the main text and the phase diagram was presented in Fig. 2.

The equations of case (ii) require, for consistency, that $4\gamma_{12}^2|\Delta_{t0}|^2\cos\alpha_{st\,0} = -\lambda^2\cos\alpha_{st\,0}$ as well as $4\gamma_{12}^2|\Delta_{t0}|^2\cos\alpha_{md\,0} = -\lambda^2\cos\alpha_{md\,0}$. These equations, on the other hand, can only be satisfied if $\cos\alpha_{st\,0} = \cos\alpha_{md\,0} = 0$, because $\lambda^2 \neq -4\gamma_{12}^2|\Delta_{t0}|^2$. In the model we are considering, $\gamma_{st} = 2\gamma_{12}$. Therefore, $\partial_{|\Delta_{t0}|}F = 0$ leads to $M_0^2 = -a_t/(\gamma_{mt}+\gamma_{st})$, if $|\Delta_t| \neq 0$. We know that $a_t > 0$ and we found numerically that $\gamma_{mt} + \gamma_{st} > 0$. Since M_0^2 cannot be negative, this is not a physical solution.

For case (iii) we have

$$\frac{\partial^2 f}{\partial\alpha_{st\,0}^2} = -2\gamma_{12}|\Delta_{s0}|^2|\Delta_{t0}|^2 - \frac{\lambda^2|\Delta_{s0}|^2}{2\gamma_{12}}, \tag{B1}$$

and $\frac{\partial^2 f}{\partial\alpha_{st0}\partial\phi_0^i} = 0$ for $\phi_0^i \neq \alpha_{st}$. Thus, $\frac{\partial^2 f}{\partial\alpha_{st\,0}^2}$ is an eigenvalue of the Hessian matrix $(\mathbb{H})_{\{\phi_0^i\}}$. In our microscopic model γ_{12} is strictly positive and thus $\partial^2 f/\partial\alpha_{st\,0}^2 < 0$. We conclude that case (iii) does not correspond to a local minimum of the free energy.

Finally, in case (iv) we obtain

$$\partial_M f = (a_m + u_m M^2 + \gamma_{ms}|\Delta_s|^2 + \gamma_{mt}|\Delta_t|^2 - \lambda^2/2\gamma_{12})M, \tag{B2}$$

and the conditions $\partial_{|\Delta_s|}f = 0$ and $\partial_{|\Delta_t|}f = 0$ lead to, respectively,

$$[a_s + u_s|\Delta_s|^2 + \gamma_{ms}M^2 + (\gamma_{st} - 2\gamma_{12})|\Delta_t|^2]|\Delta_s|^2 = 0, \tag{B3}$$

$$[a_t + \gamma_{mt}M^2 + (\gamma_{st} - 2\gamma_{12})|\Delta_s|^2]|\Delta_t|^2 = 0. \tag{B4}$$

Therefore, for our model (with $\gamma_{st} = 2\gamma_{12}$) we get $M_0^2 = -a_t/\gamma_{mt}$ (if $|\Delta_t|^2 \neq 0$), and

$$|\Delta_{t0}|^2 = \left(\lambda^2/\gamma_{st} - a_m - u_m M_0^2 - \gamma_{ms}|\Delta_{s0}|^2\right)/\gamma_{mt}, \tag{B5}$$

$$|\Delta_{s0}|^2 = -\left(a_s + M_0^2\gamma_{ms}\right)/u_s. \tag{B6}$$

For the two-band model $M_0^2 = -a_t/\gamma_{mt}$ is always positive because $\gamma_{mt} < 0$. We have computed the eigenvalues of the Hessian matrix in the regions where both $|\Delta_{s0}|^2$ and $|\Delta_{t0}|^2$ are positive and found that there is at least one negative eigenvalue. This means that the free energy is not a minimum at this solution. Thus, we conclude that, at least for the two-band model studied here, $\hat{\boldsymbol{M}}\cdot\hat{\boldsymbol{d}} = \pm 1$ and $\alpha_{st} = 0$ or π.

[1] E. Fradkin, S. A. Kivelson, and J. M. Tranquada, Rev. Mod. Phys. **87**, 457 (2015).
[2] E. Demler, W. Hanke, and S.-C. Zhang, Rev. Mod. Phys. **76**, 909 (2004).
[3] S. Sachdev, Rev. Mod. Phys. **75**, 913 (2003).
[4] D. J. Scalapino, Rev. Mod. Phys. **84**, 1383 (2012).
[5] D. K. Pratt, W. Tian, A. Kreyssig, J. L. Zarestky, S. Nandi, N. Ni, S. L. Bud'ko, P. C. Canfield, A. I. Goldman, and R. J. McQueeney, Phys. Rev. Lett. **103**, 087001 (2009).
[6] E. D. Isaacs, P. Zschack, C. L. Broholm, C. Burns, G. Aeppli, A. P. Ramirez, T. T. M. Palstra, R. W. Erwin, N. Stücheli, and E. Bucher, Phys. Rev. Lett. **75**, 1178 (1995).
[7] M.-H. Julien, H. Mayaffre, M. Horvatic, C. Berthier, X. D. Zhang, W. Wu, G. F. Chen, N. L. Wang, and J. L. Luo, Europhys. Lett. **87**, 37001 (2009).
[8] E. Wiesenmayer, H. Luetkens, G. Pascua, R. Khasanov, A. Amato, H. Potts, B. Banusch, H.-H. Klauss, and D. Johrendt, Phys. Rev. Lett. **107**, 237001 (2011).
[9] P. Marsik, K. W. Kim, A. Dubroka, M. Rössle, V. K. Malik, L. Schulz, C. N. Wang, Ch. Niedermayer, A. J. Drew, M. Willis, T. Wolf, and C. Bernhard, Phys. Rev. Lett. **105**, 057001 (2010).
[10] L. Ma, G. F. Ji, J. Dai, X. R. Lu, M. J. Eom, J. S. Kim, B. Normand, and W. Yu, Phys. Rev. Lett. **109**, 197002 (2012).
[11] P. Cai, X. Zhou, W. Ruan, A. Wang, X. Chen, D.-H. Lee, and Y. Wang, Nat. Commun. **4**, 1596 (2013).
[12] Q. Q. Ge, Z. R. Ye, M. Xu, Y. Zhang, J. Jiang, B. P. Xie, Y. Song, C. L. Zhang, P. Dai, and D. L. Feng, Phys. Rev. X **3**, 011020 (2013).
[13] Z. Li, R. Zhou, Y. Liu, D. L. Sun, J. Yang, C. T. Lin, and G.-Q. Zheng, Phys. Rev. B **86**, 180501(R) (2012).
[14] S. Kawasaki, T. Mabuchi, S. Maeda, T. Adachi, T. Mizukami, K. Kudo, M. Nohara, and G.-Q. Zheng, Phys. Rev. B **92**, 180508(R) (2015).
[15] M. Yi, Y. Zhang, Z.-K. Liu, X. Ding, J.-H. Chu, A. F. Kemper, N. Plonka, B. Moritz, M. Hashimoto, S.-K. Mo, Z. Hussain, T. P. Devereaux, I. R. Fisher, H. H. Wen, Z.-X. Shen, and D. H. Lu, Nat. Commun. **5**, 3711 (2014).
[16] W. Yu, J. S. Higgins, P. Bach, and R. L. Greene, Phys. Rev. B **76**, 020503(R) (2007).

[17] M. Yashima, S. Kawasaki, H. Mukuda, Y. Kitaoka, H. Shishido, R. Settai, and Y. Ōnuki, Phys. Rev. B **76**, 020509(R) (2007).
[18] T. Park, M. J. Graf, L. Boulaevskii, J. L. Sarrao, and J. D. Thompson, PNAS **105**, 6825 (2008).
[19] P. F. S. Rosa, J. Kang, Y. Luo, N. Wakeham, E. D. Bauer, F. Ronning, Z. Fisk, R. M. Fernandes, and J. D. Thompson, PNAS **114**, 5384 (2017).
[20] A. B. Vorontsov, M. G. Vavilov, and A. V. Chubukov, Phys. Rev. B **81**, 174538 (2010).
[21] R. M. Fernandes and J. Schmalian, Phys. Rev. B **82**, 014521 (2010).
[22] J. Schmiedt, P. M. R. Brydon, and C. Timm, Phys. Rev. B **89**, 054515 (2014).
[23] P. Ghaemi and A. Vishwanath, Phys. Rev. B **83**, 224513 (2011).
[24] Y.-M. Lu, T. Xiang, and D.-H. Lee, Nat. Phys. **10**, 634 (2014).
[25] W. Rowe, I. Eremin, A. T. Romer, B. M. Andersen, and P. J. Hirschfeld, New J. Phys. **17**, 023022 (2015).
[26] A. T. Romer, I. Eremin, P. J. Hirschfeld, and B. M. Andersen, Phys. Rev. B **93**, 174519 (2016).
[27] W. Baltensperger and S. Strässler, Phys. Kondens. Mater. **1**, 20 (1963).
[28] L. N. Bulaevskii, A. I. Rusinov, and M. Kulic, J. Low Temp. Phys. **39**, 255 (1980).
[29] M. J. Nass, K. Levin, and G. S. Grest, Phys. Rev. Lett. **46**, 614 (1981).
[30] K. Machida, J. Phys. Soc. Jpn. **50**, 2195 (1981).
[31] A. M. Gabovich and A. S. Shpigel, J. Phys. F **14**, 3031 (1984).
[32] M. Gulacsi and Zs. Gulacsi, Phys. Rev. B **33**, 6147 (1986).
[33] M. Kato and K. Machida, Phys. Rev. B **37**, 1510 (1988).
[34] Y. Zhang, E. Demler, and S. Sachdev, Phys. Rev. B **66**, 094501 (2002).
[35] T. Das, R. S. Markiewicz, and A. Bansil, Phys. Rev. B **77**, 134516 (2008).
[36] V. Stanev, J. Kang, and Z. Tesanovic, Phys. Rev. B **78**, 184509 (2008).
[37] G. C. Psaltakis and E. W. Fenton, J. Phys. C **16**, 3913 (1983).
[38] H.-D. Chen, O. Vafek, A. Yazdani, and S.-C. Zhang, Phys. Rev. Lett. **93**, 187002 (2004).
[39] D. F. Agterberg and H. Tsunetsugu, Nat. Phys. **4**, 639 (2008).
[40] E. Berg, E. Fradkin, and S. A. Kivelson, Phys. Rev. B **79**, 064515 (2009).
[41] V. Cvetkovic and O. Vafek, Phys. Rev. B **88**, 134510 (2013).
[42] M. Murakami and H. Fukuyama, J. Phys. Soc. Jpn. **67**, 2784 (1998).
[43] B. Kyung, Phys. Rev. B **62**, 9083 (2000).
[44] A. Aperis, G. Varelogiannis, P. B. Littlewood, and B. D. Simons, J. Phys.: Condens. Matter **20**, 434235 (2008).
[45] D. F. Agterberg, M. Sigrist, and H. Tsunetsugu, Phys. Rev. Lett. **102**, 207004 (2009).
[46] K.-i. Hosoya and R. Ikeda, Phys. Rev. B **95**, 224513 (2017).
[47] K. Kuboki and K. Yano, J. Phys. Soc. Jpn. **81**, 064711 (2012).
[48] A. Hinojosa, R. M. Fernandes, and A. V. Chubukov, Phys. Rev. Lett. **113**, 167001 (2014).
[49] R. Balian and N. R. Werthamer, Phys. Rev. **131**, 1553 (1963).
[50] A. J. Leggett, Rev. Mod. Phys. **47**, 331 (1975).
[51] A. P. Mackenzie and Y. Maeno, Rev. Mod. Phys. **75**, 657 (2003).
[52] M. Marciani, L. Fanfarillo, C. Castellani, and L. Benfatto, Phys. Rev. B **88**, 214508 (2013).
[53] A. J. Leggett, Phys. Rev. **147**, 119 (1966).
[54] R. M. Fernandes, A. V. Chubukov, J. Knolle, I. Eremin, and J. Schmalian, Phys. Rev. B **85**, 024534 (2012).
[55] N. D. Mermin and H. Wagner, Phys. Rev. Lett. **17**, 1133 (1966).